supported by the Director, Office of Energy Research, Office of Basic Energy Sciences, Chemical Science Division of the U.S. Department of Energy under Contract No. DE-Ac03-67SF00098. Additional support was provided by the U.S.-Yugoslav Joint Fund for Scientific and Technological Cooperation, in association with the National Science Foundation under Grant No. JF947. That part of the work carried out at the Jožef Stefan Institute was supported by the Research Community of Slovenia.

Experimental and Theoretical Aspects of the Formation of Radical Cations from Tripyrrolidinobenzenes and Their Follow-Up Reactions[1]

Franz Effenberger,*,† Wolf-Dieter Stohrer,*,§ Karl-Ernst Mack,† Friedrich Reisinger,† Walter Seufert,† Horst E. A. Kramer,‡ Rudolf Föll,‡ and Ekehardt Vogelmann‡

Contribution from the Institut für Organische Chemie and the Institut für Physikalische Chemie der Universität Stuttgart, Pfaffenwaldring 55, 7000 Stuttgart 80, Federal Republic of Germany, and Institut für Organische Chemie der Universität Bremen, 2800 Bremen, Federal Republic of Germany. *Received September 14, 1989*

Abstract: Tripyrrolidinobenzene radical cations ($\mathbf{1}^{\bullet+}$), obtained from the corresponding arenes by oxidation with silver nitrate, are specially stabilized and thus allow specific reaction pathways of arene radical cations to be investigated separately and individually. Radical cations $\mathbf{1}^{\bullet+}$, for instance, generated under exclusion of oxygen, undergo dimerization to **2**, or they abstract hydrogen from the solvent to form **3**. In a pure oxygen atmosphere, the O_2 reaction products **6** and **7** are formed, respectively, either exclusively or together with **2** and **3**. Kinetic measurements give the following order of reactivity for these individual processes: reaction with O_2 > dimerization (initial $[\mathbf{1}^{\bullet+}]$ being ca. 10^{-4} M under flash photolysis conditions) > H-abstraction from solvent. The changes in the product spectrum upon modification of the reaction conditions are in accord with the kinetic results. The dimeric σ complexes **2** show surprisingly facile dissociation into two radical cations, two ($\mathbf{1}^{\bullet+}$), with a much higher dissociation rate for the alkyl derivatives **2b–d** than for **2a**. Dissociation is enhanced substantially by light or in the presence of π donors. Individual product formation, rate of reactions of the radical cations $\mathbf{1}^{\bullet+}$, and photochemical cleavage of the dimeric σ complexes **2** can be rationalized, by qualitative and quantitative MO considerations, in terms of their relative frontier orbital energies.

The yield of dimeric σ complexes **2** from the oxidation of 1,3,5-tripyrrolidin-1-ylbenzenes **1** is extremely dependent upon the effective reaction conditions.[1] Alkyl-substituted tripyrrolidinobenzenes, especially, have to be oxidized under absolute exclusion of light, and the reaction mixtures have to be worked up very quickly to obtain reproducible results and satisfactory yields of defined products.[1] This is due to different reaction pathways open to the intermediate radical cations $\mathbf{1}^{\bullet+}$ which themselves may be formed either directly by oxidation of the triaminobenzenes **1** or by dissociation of the dimeric σ complexes **2** (see Scheme I). In the present paper, we report a detailed study of the electronic structure, physical properties, and chemical reactions of tripyrrolidinobenzene radical cations which allow the "preparation" of individual pathways from the manifold of secondary reactions, typical and/or feasible for aromatic radical cations in general.[2]

Oxidation of 1,3,5-Tripyrrolidin-1-ylbenzene (1) with Silver Nitrate under Various Conditions

In contrast to our earlier report,[1] oxidation of **1a–d** by silver nitrate was now carried out in the dark, at ambient temperature, with painstaking exclusion of oxygen. In one extreme, the oxidant (in CH_3CN/CH_2Cl_2 solution) was added, within 10 s, to a CH_2Cl_2 solution of **1**, and workup was initiated after 10 min. In the other extreme, addition of the oxidant was spread over 6 h, under otherwise identical conditions, with rapid workup of the reaction mixtures in each case. A mixture of the respective monomeric and dimeric σ complexes **2** and **3** was obtained for both extreme conditions, although with varying percentages (see Scheme I, Table I). Due to the kinetic lability of the products (vide infra), the composition of the crude crystalline mixtures was determined by ^1H NMR. Oxidation of 1-methyl-2,4,6-tripyrrolidin-1-ylbenzene (**1b**) gave, besides **2b** and **3b**, an additional 10% of the 1-methylene-2,4,6-tripyrrolidin-1-ylcyclohexadienylium complex **5** by deprotonation of the radical cation $\mathbf{1b}^{\bullet+}$ and further oxidation of the benzyl radical thus formed.[3]

Deprotonation by methoxide of the crude product mixtures gave mixtures of **1** and the respective biphenyls **4**; the combined yield of **1** and **4** corresponds to the amount of **1** employed in oxidation. One may conclude, then, that the only reaction channels open to the radical cations $\mathbf{1}^{\bullet+}$ in the absence of oxygen are dimerization and hydrogen abstraction from the solvent (with the exception of the 10% side reaction of **1b** mentioned above).

Slow oxidation of **1a–d** (2–6 h, see above) in a pure oxygen atmosphere afforded, under otherwise identical conditions, only products derived from an initial reaction of $\mathbf{1}^{\bullet+}$ with molecular oxygen. Thus, the 1-oxo-2,4,6-tripyrrolidin-1-ylcyclohexadienylium complex **6a** was obtained from **1a**, and the 1,1′-dialkyl-2,2′,4,4′,6,6′-hexapyrrolidin-1-yldicyclohexadienylium

† Institut für Organische Chemie Universität Stuttgart.
‡ Institut für Physikalische Chemie Universität Stuttgart.
§ Institut für Organische Chemie der Universität Bremen.

(1) Aminobenzenes 20. For part 19 see: Effenberger, F.; Mack, K. E.; Niess, R.; Reisinger, F.; Steinbach, A.; Stohrer, W.-D.; Stezowski, J. J.; Rommel, I.; Maier, A. *J. Org. Chem.* **1988**, *53*, 4379.
(2) Effenberger, F.; *Acc. Chem. Res.* **1989**, *22*, 27.
(3) (a) Parker, V. D. *Acta Chem. Scand. B* **1985**, *39*, 227. (b) Edlund, O.; Kinell, P.-O.; Lund, A.; Shimizu, A. *J. Chem. Phys.* **1967**, *46*, 3679. (c) Badger, B.; Brocklehurst, B. *Trans. Farad. Soc.* **1967**, *46*, 3679. (d) Ekstrom, A. *J. Chem. Phys.* **1970**, *74*, 1705. (e) Bewick, A.; Edward, G. J.; Mellor, J. M. *Tetrahedron Lett.* **1975**, 4685. (f) Kira, A.; Imamura, M. *J. Phys. Chem.* **1979**, *83*, 2267.

0002-7863/90/1512-4849$02.50/0

Scheme I

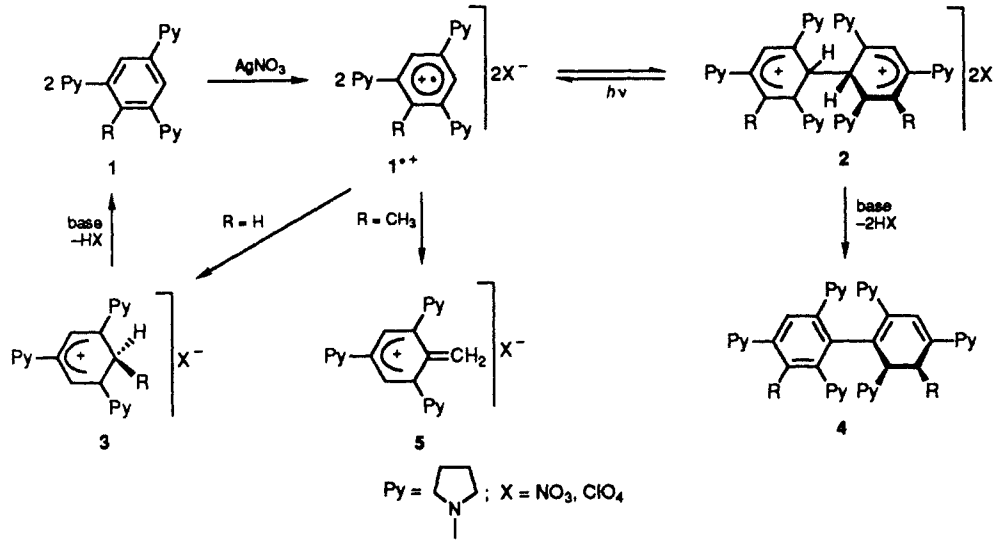

Scheme II

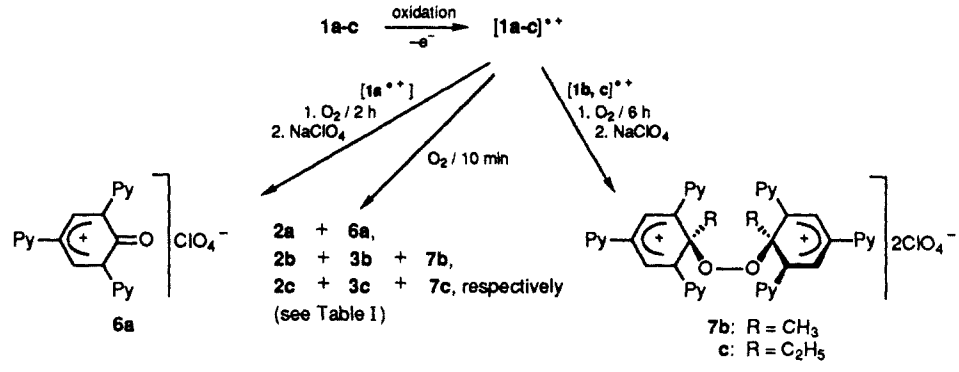

Table I. Oxidation of 1,3,5-Tripyrrolidin-1-ylbenzenes **1** with Exclusion of Light

(A) In a Pure Dry Nitrogen Atmosphere

			products[a]			
1	R	method[b]	**2**	2,2′,4,4′,6,6′-hexapyrrolidin-1-yl-1,1′-bicyclohexadienylium complex	**3**	2,4,6-tripyrrolidin-1-ylcyclohexadienylium complex
1a	H	A	**2a**	unsubstituted (100)		
1b	CH_3	A	**2b**	3,3′-dimethyl- (66)	**3b**	1-methyl- (23)[c]
1c	C_2H_5	A	**2c**	3,3′-diethyl- (85)	**3c**	1-ethyl- (15)
1d	$CH(CH_3)_2$	A	**2d**	3,3′-diisopropyl- (80)	**3d**	1-isopropyl- (20)
1a	H	B	**2a**	unsubstituted (80)	**3a**	unsubstituted (20)
1b	CH_3	B	**2b**	3,3′-dimethyl- (37)	**3b**	1-methyl- (53)[d]
1c	C_2H_5	B	**2c**	3,3′-diethyl- (50)	**3c**	1-ethyl- (50)
1d	$CH(CH_3)_2$	B	**2d**	3,3′-diisopropyl- (38)	**3d**	1-isopropyl- (65)

(B) In an Oxygen Atmosphere (Method A)

	products[a]				
1	**2**	**3**	**6a**[e]	**7**	2,2′,4,4′,6,6′-hexapyrrolidin-1-yl-1,1′-bicyclohexadienylium peroxide complex
1a	**2a** (60)		(40)		
1b	**2b** (45)	**3b** (15)		**7b**	3,3′-dimethyl- (40)
1c	**2c** (60)	**3c** (10)		**7c**	3,3′-diethyl- (30)

[a] Numbers in parentheses are percentage composition, determined by ^1H NMR. [b] Addition of $AgNO_3$ in CH_3CN/CH_2Cl_2 within 10 s and rapid workup initiated after 10 min (method A), within 6 h and subsequent rapid workup (method B). [c] Additionally 1-methylene-2,4,6-tripyrrolidin-1-ylcyclohexadienylium complex **5** (11%). [d] Additionally **5** (10%). [e] 1-Oxo-2,4,6-tripyrrolidin-1-ylcyclohexadienylium complex.

peroxide complexes **7b,c**, from **1b,c**. Rapid addition (20 s and 10 min subsequent stirring; see above) of the oxidant to solutions of **1a–c** in a pure oxygen atmosphere afforded, apart from the oxygen-containing products **6a** and **7b,c**, respectively, once more both dimeric σ complexes **2** and hydrogen abstraction products **3** (Scheme II, Table I).

6a was precipitated from the aqueous reaction mixture by addition of sodium perchlorate in 94% crude yield; recrystallization from methanol afforded 76% analytically pure, black-green crystals of **6a**. The peroxide complexes **7b,c** could be isolated in pure form only by gel chromatography and subsequent precipitation as the perchlorates, with a concomitant sharp decrease in overall yield.

Scheme III

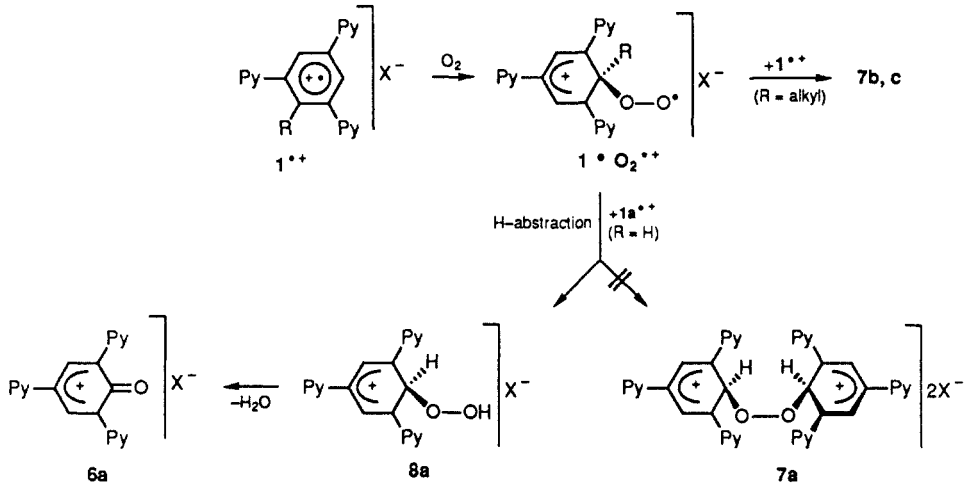

Table II. Dissociation of the Dimeric σ Complexes **2a–d** (Diperchlorates) in CH_2Cl_2 with Exclusion of Light

educts						products[a]		
2 (R)	+ 1a (mmol)	under N_2 or O_2	time	temp, °C	2	3	7
2a[b] (R = H)	–	N_2	1 h	80	**2a** (95)	**3a** (5)	–
	1.0	N_2	3 h	80	–	**3a** (100)	–
	1.0	O_2	3 h	80	–	**3a** (75)	–[c]
2b[d] (R = CH_3)	–	N_2	40 days	25	–	**3b** (100)	–
	1.5	N_2	6 h	25	**2b** (7)	**3b** (93)	–
	1.5	O_2	6 h	25	**2b** (22)	**3b** (35)	**7b** (43)
2c (R = C_2H_5)	–	N_2	50 days	25	–	**3c** (100)	–
	1.5	N_2	10 h	25	–	**3c** (100)	–
	1.5	O_2	10 h	25	**2c** (4)	**3c** (73)	**7c** (23)
2d (R = $CH(CH_3)_2$)	–	N_2	100 days	25	–	**3d** (100)	–
	1.5	N_2	3 days	25	–	**3d** (100)	–
	1.5	O_2	3 days	25	**2d** (12)	**3d** (72)	**7d** (16)

[a] Numbers in parentheses are percentage composition, determined by ^1H NMR. [b] In CH_3CN. [c] Additionally **6a** (25%). [d] Bis(tetrafluoroborate).

For the isopropyl derivative **1d**, the corresponding peroxide complex **7d** could not be isolated in pure form and could not even be characterized unequivocally by ^1H NMR.

The compounds **7** derived from aromatic radical cations and molecular oxygen represent the first σ complex intermediates with a peroxy linkage; their unexpectedly high thermal stability must be attributed to a special structural principle.[4] This is reflected also in the EI mass spectrum of **7c** which displays the radical cation formed by homolytic cleavage of the peroxide bond (m/z 329), together with the radical cation formed by expulsion of O_2 (m/z 313).

The different product spectrum obtained upon oxidation in an O_2 atmosphere may be rationalized as outlined in Scheme III: In the first step, the radical cations **1**$^{\bullet+}$ add molecular oxygen to the peroxy radical intermediates **1**$\cdot O_2^{\bullet+}$.[5] In the case of **1b–d**$^{\bullet+}$, the aryl radical cations are sufficiently stabilized to build up a steady-state concentration which is high enough to allow for a bimolecular, radical combination with the peroxy radicals, forming the stable peroxides **7b–d**. Due to its instability, the steady-state concentration of **1a**$^{\bullet+}$ is so low that hydrogen abstraction, which is first-order with respect to **1a**$\cdot O_2^{\bullet+}$, prevails over the second-order radical combination with **1a**$^{\bullet+}$. The hydroperoxide **8a** thus formed eliminates H_2O to give the final oxo product **6a**. Two results support this mechanistic rationale: First, upon oxidation of **1a**, deuterated in all three aryl positions, the water formed consists of 13% D_2O, 40% HOD, and 47% H_2O. Second, neither H_2 nor D_2 can be detected in the oxidation of **1a** or d_3-**1a** which would have to be formed if the reaction proceeded via **7a** as intermediate (see Scheme III).

Dissociation of Dimeric σ Complexes 2 into Two Radical Cations 1$^{\bullet+}$ and Their Follow-Up Reactions

The radical cations **1**$^{\bullet+}$, formed in the first step of triaminobenzene oxidation, can form charge-transfer complexes with excess educt **1**.[6,7] Thus, one might visualize a different reactivity pattern for radical cations formed by direct oxidation and for those generated by dissociation of the dimeric σ complexes **2**. For direct comparison with the silver nitrate oxidation, we have carried out the dissociation reactions also with exclusion of light. Especially for **2a**, this is a very slow process. We have found, however, that dissociation is enhanced not only by light, but also by the addition of π donors such as **1a**. Table II summarizes our findings for the dissociation of the dimeric σ complexes **2a–d** under various conditions.

The following conclusions can be drawn by comparing the results listed in Table II with those in Table I.

(i) Radical cations **1**$^{\bullet+}$ from the oxidation of aminobenzenes **1** can either add molecular oxygen ($k_{O_2} \rightarrow$ **6**, **7**), abstract hydrogen, e.g. from the solvent ($k_{H\text{-abstr}} \rightarrow$ **3**), or dimerize via radical combination ($k_{dim} \rightarrow$ **2**). From the product spectrum in the case of slow oxidation, the following gradations for the individual processes may be derived: Reaction with O_2 > dimerization (initial [**1**$^{\bullet+}$] being ca. 10^{-4} M under flash photolysis conditions) > H-abstraction from solvent.

(ii) Dissociation of the dimeric σ complexes **2** into two radical cations **1**$^{\bullet+}$ appears substantially accelerated in the presence of light or π donor molecules. The product spectra for the secondary

(4) Effenberger, F.; Reisinger, F.; Schönwälder, K. H.; Bäuerle, P.; Stezowski, J. J.; Jogun, K. H.; Schöllkopf, K.; Stohrer, W.-D. *J. Am. Chem. Soc.* **1987**, *109*, 882.

(5) Nelsen, S. F.; Akaba, R. *J. Am. Chem. Soc.* **1981**, *103*, 2096.

(6) (a) Meot-Ner, M. *J. Phys. Chem.* **1980**, *84*, 2724. (b) Meot-Ner, M.; El-Shall, M. S. *J. Am. Chem. Soc.* **1986**, *108*, 4386. (c) El-Shall, M. S.; Kafafi, S. A.; Meot-Ner, M.; Kertesz, M. *J. Am. Chem. Soc.* **1986**, *108*, 4391.

(7) (a) Molosevich, S. A.; Saichek, K.; Hinchey, L.; England, W. B.; Kovacic, P. *J. Am. Chem. Soc.* **1983**, *105*, 1088. (b) Aalstad, B.; Ronlan, A.; Parker, V. D. *Acta Chem. Scand. B* **1983**, *37*, 467. (c) Chandra, A. K.; Bhanuprakash, K.; Bhasu, V. C. J.; Srikanthan, D. *Mol. Phys.* **1984**, *52*, 733.

Table III. Half-Periods of Dissociation of the Dimeric σ Complexes **2b–d** (Diperchlorates)

(A) Determined UV Spectroscopically in ~1.5 × 10^{-5} M CH_3CN Solution (20 °C, with Absolute Exclusion of Oxygen)

	2b (R = Me)	2c (R = Et)	2d (R = *i*-Pr)
with exclusion of light	2.5 h	12 h	204 h
with intermittent exposure of daylight	80 s	85 s	105 s

(B) Determined by ^1H NMR in 0.1 M $CD_3CN/CDCl_3$ (1:1 v/v) Solution (30 °C, with Strict Exclusion of Both Light and Oxygen) in the Presence of π Arene Donors (0.15 mmol)

π donor added	2b (h)	2c (h)	2d (h)
none	17	48	276
1a (R = H)	0.5	7	108
1b (R = CH_3)	1.5	*a*	*a*
1c (R = C_2H_5)	*a*	16	*a*
1,3,5-tripiperidin-1-ylbenzene	1.5	26	252

[a] Not determined.

reactions of the radical cations generated in this manner are comparable to that obtained for *slow* oxidation.

Kinetic Investigation of the Dissociation of Dimeric σ Complexes 2 and of the Secondary Reactions of Generated Radical Cations $1^{\bullet+}$

As demonstrated above, only two reaction channels are open to radical cations $1^{\bullet+}$ generated by dissociation of the dimeric σ complexes **2** under exclusion of oxygen, i.e. recombination to **2** or hydrogen abstraction to **3**. It is possible, therefore, to infer the actual rate of dissociation, $2 \rightarrow 2(1^{\bullet+})$, from the rate of formation of **3**, with dependence on the alkyl substituent R (see Scheme I). The formal kinetics of the dissociation reaction in fact confirm the mechanism postulated for the cleavage of **2**. If

$$K = \frac{k_{diss}}{k_{rec}} = \frac{[1^{\bullet+}]^2}{[2]}$$

$$\frac{-d[2]}{dt} = 2k[1^{\bullet+}];$$

$$-\tfrac{1}{2}\frac{d[2]}{dt} = k\sqrt{K}\sqrt{[2]}$$

$$\sqrt{[2]_0} - \sqrt{[2]} = k\sqrt{K}t$$

($\sqrt{[2]_0} - \sqrt{[2]}$) is plotted against t, a linear correlation is obtained from about 20% turnover onward. (The faster reaction at the outset probably is due to the time necessary for establishing the steady-state dissociation/recombination equilibrium.) Thus, the following effective rate constants $k\sqrt{K}$ were determined: 300 × 10^{-9} for **2b**, 23 × 10^{-9} for **2c**, 3.3 × 10^{-9} (mol $L^{-1})^{1/2}$ s^{-1} for **2d**. Under the influence of light, the reaction $2 \rightarrow 3$ is so much faster that the difference in rate between **2b,c,d** is washed out, and a value of 1.5 × 10^{-5} is found for $k\sqrt{K}$ for all three compounds. From these UV measurements, half-life times were determined for the three dimeric σ complexes **2b–d** under strict exclusion of light, as well as with intermittent exposure to daylight[8a] (see Table IIIA).

Table III gives the half-life times of the dimeric σ complexes **2b–d** in the absence of light, but with either **1a–c** or 1,3,5-tripiperidin-1-ylbenzene added as π donors; these values were determined solely by ^1H NMR spectroscopy (Table IIIB). For **2a**, dissociation is too slow at ambient temperature even in the presence of π donors to determine a half-decay time.

The acceleration of the dissociation reaction by π donor molecules (see Table IIIB) correlates with the oxidation potential of these donors, i.e. the reaction is faster in the presence of 1,3,5-tripyrrolidin-1-ylbenzene than 1,3,5-tripiperidin-1-ylbenzene ($E_{1/2}$ = 0.38 vs 0.54 V).[8b,c] The enhancement of the dissociation rate decreases in the series **2b > 2c > 2d**, due probably to diminished CT interaction (for steric reasons) of the alkyl-substituted σ complexes **2** with the π donors.

Scheme IV

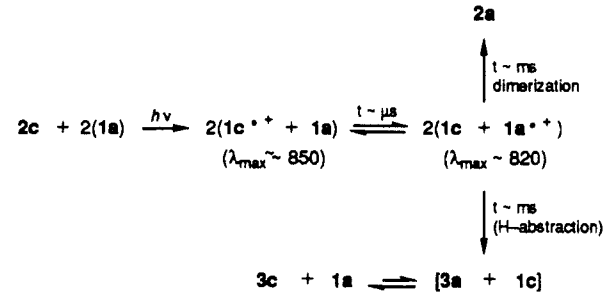

Absolute rate constants were determined for the individual secondary processes of $1c^{\bullet+}$ in order to obtain more detailed information on structure/reactivity correlations for aromatic radical cations. The radical cations were generated, first, by conventional flash photolysis (excitation wavelength > 400 nm),[9a] and, second, by laser pulses at 460 nm.[9b] The dimeric σ complex **2c** therefore is selectively excited in the longest wavelength absorption band. The quantum yields for the photolysis of **2c** are extremely high ($\phi \leq 1$).

The kinetics of the follow-up reactions of the radical cations $1c^{\bullet+}$ generated by flash photolysis from **2c** are easily monitored from their characteristic long-wavelength absorption (λ_{max} = 850 nm)[3,10] by time-resolved absorption spectroscopy. The predominant process of the radical cations $1c^{\bullet+}$ is second-order recombination (dimerization) to **2c**. First-order hydrogen abstraction to **3c** is a minor process. Recombination can likewise be established directly from fading spectra in the shorter wavelength region. The following rate constants were determined for the individual reactions of $1c^{\bullet+}$: k_{dim} = (1.25–2.0) × 10^4 L mol^{-1} s^{-1}, $k_{H\text{-}abstr}$ = 0.05–0.3 s^{-1}.

The reaction with oxygen is even faster than dimerization $k_{O_2}[O_2]$ = 5.4 × 10^2 s^{-1} (for $[O_2] \approx 0.47 \times 10^{-3}$ mol l^{-1}, air-saturated solution).[11]

The kinetics of the photochemical cleavage of **2c** were monitored once with **1c** added to the reaction mixture and once with **1a**, to probe for an eventual CT interaction between $1c^{\bullet+}$ and the triaminobenzenes **1**. Addition of **1c** did not result in any significant change of either the spectral behavior or the individual rates for the photolysis of **2c**: k_{dim} = (1.0–2.0) × 10^4 L mol^{-1} s^{-1}; $k_{H\text{-}abstr}$ = 0.23–0.51 s^{-1}. If, however, photolysis of **2c** is carried out in the presence of **1a**, a completely different reaction pattern emerges. First, a very short-lived species appears (~10 μs; λ_{max} = 850 nm), with an electron spectrum comparable to that of $1c^{\bullet+}$. This first intermediate is transformed into a second one with longest wavelength absorption at 820 nm, which, in the millisecond range, reacts to form the products finally isolated. This second intermediate can only be a radical cation since neither the corresponding arene nor the respective σ complex absorbs in this spectral region.

A closed evaluation of these kinetic processes over the total reaction time was not possible, but the individual time dependencies could be simulated with fair correlation by assuming the two-step reaction outlined in Scheme IV. The dimeric σ complex **2c** is

(8) (a) Mack, K. E. Dissertation, Universität Stuttgart, 1974. (b) Schirmer, U. Dissertation, Universität Stuttgart, 1973. (c) Effenberger, F.; Fischer, P.; Schoeller, W. W.; Stohrer, W.-D. *Tetrahedron* **1978**, *34*, 2409.

(9) (a) Kramer, H. E. A.; Maute, A. *Photochem. Photobiol.* **1972**, *15*, 7. (b) Ulrich, T.; Steiner, U. E.; Föll, R. E. *J. Phys. Chem.* **1983**, *87*, 1873.

(10) (a) Hausser, K. H.; Murrell, J. N. *J. Chem. Phys.* **1957**, *27*; 500. (b) Takemoto, K.; Nakayama, S.; Suzuki, K.; Ooshika, Y. *Bull. Chem. Soc. Jpn.* **1968**, *41*, 1974. (c) Kimura, K.; Yamada, H.; Tsubomura, H. *J. Chem. Phys.* **1968**, *48*, 440.

(11) The solubility of O_2 in DMSO, calculated for the molar fraction (Clever, H. L.; Battino, R. In *Techniques of Chemistry*; Weissberger, A., Ed.; Vol. VIII, Solutions and Solubilities, Dack, M. R. J., Ed.; Part I; Wiley-Intersciences: New York, 1975; pp 327–377), was taken as good approximation of the solubility of O_2 in CH_3CN.

dissociated in the established manner into two radical cations $\mathbf{1c}^{\bullet+}$, which, in the microsecond range, undergo electron transfer with **1a**, yielding, in turn, **1c** and $\mathbf{1a}^{\bullet+}$. This alternate radical cation $\mathbf{1a}^{\bullet+}$, for sterical reasons, reacts 1000 times faster than $\mathbf{1c}^{\bullet+}$ (hydrogen abstraction of $\mathbf{1c}^{\bullet+}$ occurs in the second range, see above). The quasi-equilibrium between the two radical cations, therefore, is depleted only by follow-up reactions of $\mathbf{1a}^{\bullet+}$ which are in the millisecond range. This mechanistic sequence, derived from the spectroscopic results, is confirmed by the product spectrum obtained from photolysis of the dimeric σ complex **2c** (as perchlorate) run on a preparative scale in the presence of **1a**. In these experiments, 31% each of the dimeric complexes **2a** (as perchlorate) and 1-ethyl-2,4,6-tripyrrolidin-1-ylbenzene (**1c**) were obtained along with 19% monomeric σ complex **3c** and 20% 1,3,5-tripyrrolidin-1-ylbenzene (**1a**). Monomeric σ complex **3a** could not be detected even in traces. We suppose, therefore, that **3a** formed by $\mathbf{1a}^{\bullet+}$ abstracting a hydrogen from the solvent is deprotonated by the stronger base **1c**,[12] formed at the same time (see Scheme IV), thus regenerating **1a**.

Theoretical Interpretation of Experimental and Kinetic Data

Hyperconjugative weakening of the central C–C bond,[1] combined with electrostatic repulsion between the two positively charged cyclohexadienylium subunits provides a straightforward, prima facie rationale for the facile *thermal* cleavage of the dimeric σ complexes **2**. In the proper conformation, these complexes present ideal prerequisites for intramolecular excimer formation. Thus, one would expect their dissociation tendency to be less in the electronically excited state than in the ground state, i.e. *photochemical* cleavage to be impeded, and not enhanced as found experimentally.

Closer inspection reveals, however, that coupling of the two cyclohexadienylium π systems through the central C–C bond, and not alone through-space interaction, is of crucial importance for the electronic configuration, and thence the chemical reactivity of the dimeric σ complexes **2**. They represent ideal models, therefore, for demonstrating competitive through-space/through-bond interaction.[13]

Figure 1 gives a molecular orbital correlation diagram for the dimeric σ complexes **2** without the pyrrolidino groups for clarity of presentation. The five π orbitals each of the two cyclohexadienylium subunits (column A) are split, by pure through-space interaction, into pairs of stabilized (π_{1-5}^{+}) and destabilized (π_{1-5}^{-}) combinations. In the following, discussion shall be confined more or less to the HOMOs and LUMOs of the dimeric σ complexes, i.e. $\pi_2^{\pm}$ and $\pi_3^{\pm}$. Character (stabilization/destabilization) and extent of the through-space interaction, which gives rise to the splitting into $\pi_2^{\pm}$, $\pi_3^{\pm}$, are extremely sensitive to the conformation about the central σ bond. This conformation can be characterized in terms of the torsional angle α and an interplanar bending angle β.

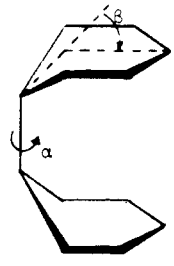

$\alpha = 0°$ for two eclipsed rings
$\beta = 0°$ for the sp^3 carbon in the plane of the five cyclohexadienylium C atoms

One of the through-space combinations of the LUMO set $\pi_3^{\pm}$ is symmetrical with respect to a C_2 axis which is orthogonal to the central σ bond, as shown by the schematical Newman projection in Figure 2. This symmetrical combination is bonding between the two cyclohexadienylium π systems for all torsional angles α, and the corresponding antisymmetrical combination is antibonding over the whole range of 180°. The qualitative splitting pattern between these two through-space combinations, also shown in Figure 2, is confirmed numerically by EH calculations and still holds if the bending angle β is varied from 0 to 40°. The absolute value of the splitting energy of course increases with larger interplanar angles β.

If the same argument is applied to the HOMO set $\pi_2^{\pm}$, the through-space combination, which is symmetrical with respect to the C_2 axis, comes out as antibonding between the two cyclohexadienylium π systems for angles $\alpha \leq 60°$, and as bonding for $\alpha \geq 60°$. The reverse behavior holds for the antisymmetrical combination so that, in the region of $\alpha \approx 60°$, the energies of the two highest occupied orbitals cross. Through-bond interaction, on the other hand, is but moderately dependent on the interplanar and independent of the torsional angle. Thence, conformations with small through-space splitting (e.g. $\alpha \approx 60°$ and $\alpha > 150°$ for $\pi_3^{\pm}$, see Figure 2) are predestined for dominant through-bond interaction.

In Figure 1, through-bond coupling between the two π systems is taken into account by mixing the central C–C bond σ,σ^* orbitals with the through-space combinations (C → D). This leaves $\pi_2^{\pm}$ and $\pi_4^{\pm}$ virtually unchanged; the remaining through-space combinations, on the other hand, strongly mix with either σ or σ^*. Whether the original, through-space-determined order of the two LUMOs is reversed then, as shown in Figure 1 (column D), depends on the actual values of through-space and through-bond splitting. Independent of this relative LUMO order, the bonding σ orbital mixes into the unoccupied combinations π_3^{+} and π_5^{+}, as shown by a comparison between columns C and D in Figure 1. The concomitant transfer of electron density from σ to π_3^{+}, π_5^{+} weakens the central C–C σ bond. Inversely, mixing of the occupied π_1^{-} into the antibonding σ^* orbital results in a partial transfer of electron density from the bonding π_1^{-} into the antibonding σ^* orbital and thus likewise weakens the central C–C bond. This is the MO theoretical rationale for the "hyperconjugative" weakening of this bond in the dimeric σ complexes, mentioned above, which facilitates, apart from the electrostatic repulsion between the two positively charged subunits, the thermal cleavage of the dimeric σ complexes **2** into two radical cations $\mathbf{1}^{\bullet+}$.

Photoreactivity in condensed phase is governed, in terms of the photochemical dogma, by the lowest electronically excited state which can be described qualitatively in a single-determinant model, by raising one electron from HOMO to LUMO. The question of which is the LUMO of the dimeric σ complexes **2**, i.e. of the relative energetic order of the two lowest unoccupied orbitals, thus becomes crucially important for the photochemical behavior of **2**. EH calculations have proven reliable for evaluating, more or less quantitatively, the delicate interplay between through-bond and through-space interaction. We have calculated, therefore, the relative energetic order of the two lowest unoccupied orbitals of the dimeric σ complexes, $(\pi_3^{+} - \sigma)$ and $(\pi_3^{-} + \sigma^*)$, as a function of the two conformational angles α and β; the results are presented graphically in Figure 3. The "classical" order, i.e. $(\pi_3^{+} - \sigma)$ energetically lower than $(\pi_3^{-} + \sigma^*)$, is retained only for rather improbable conformations, through-bond interaction dominating for all "energetically reasonable" conformations. For two dimeric σ complexes, the following conformations were determined by X-ray crystallography:[1] **2a**, $\alpha = 65°$, $\beta \sim 40°$; **2c**, $\alpha = 163°$, $\beta \sim 35°$. It is highly satisfying to note that these two conformations lie right within those regions where through-bond-determined splitting of the two LUMOs is at a maximum (see Figure 3). Their relative order, as given in Figure 1 (column D), thus appears justified both theoretically *and* experimentally.

In the first electronically excited state, one electron is promoted from an orbital, which is antibonding between the two rings and has virtually no σ/σ^* character admixed, into a LUMO with pronounced σ^* character. This further favors severance of the central C–C bond, weakened a priori by hyperconjugative in-

(12) Knoche, W.; Schoeller, W. W.; Schönäcker, R.; Vogel, S. *J. Am. Chem. Soc.* **1988**, *110*, 7484.
(13) Hoffmann, R. *Acc. Chem. Res.* **1971**, *4*, 1.

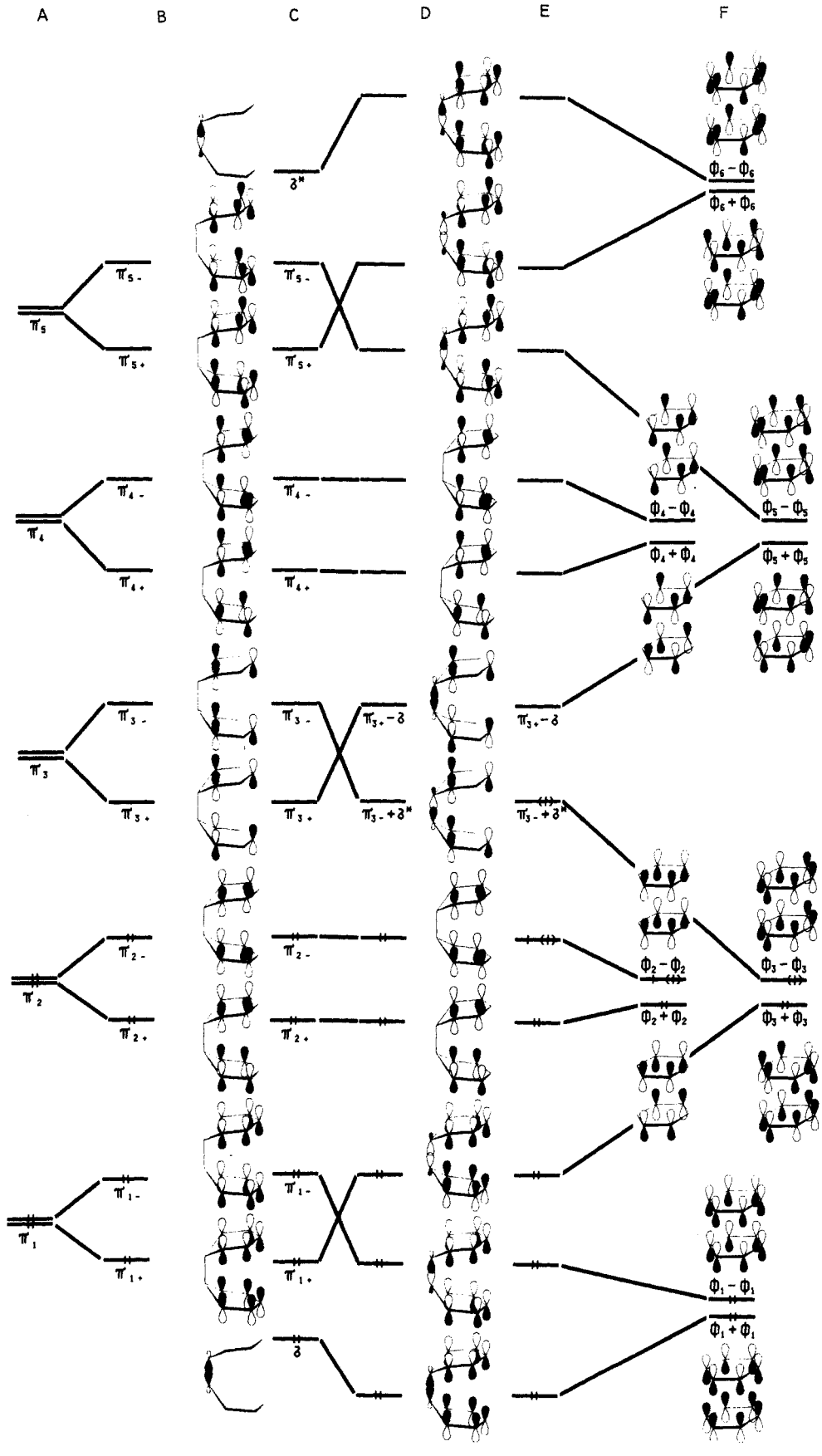

Figure 1. Schematic orbital interaction diagram for the dimeric σ complex "π" orbitals (for clarity of presentation without the amino substituents) and, at the right, correlation diagram for the dissociation of a dimeric σ complex into two benzene radical cations. Column A: π orbitals of two noninteracting cyclohexadienylium subunits. Column B: π orbitals of the dimeric σ complex with through-space splitting only. Column C: through-space splitting order (Column B) together with the σ,σ^* orbitals of the central C–C bond. Columns D, E: orbitals resulting after incorporation of through-bond interaction. Column F: the different configurations of two, interacting, Jahn–Teller distorted, benzene radical cations.

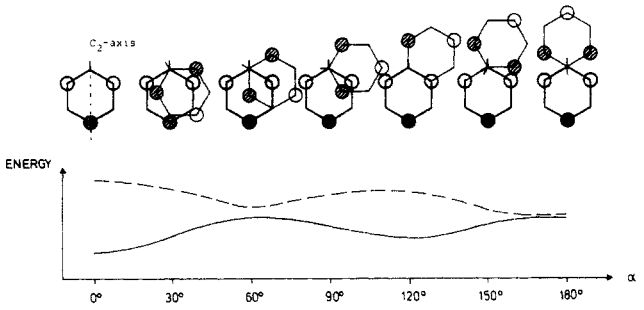

Figure 2. Schematic representation of that LUMO (π_3 orbital) through-space combination of the two cyclohexadienylium subunits which is symmetrical with respect to the C_2 axis, with torsion about the central C–C σ bond in 30° steps (top). Dependence of the energetical splitting of the two LUMO combinations π_3^+ and π_3^- on the torsional angle α (bottom): symmetrical combination (—) with respect to C_2, antisymmetrical combination (- - -).

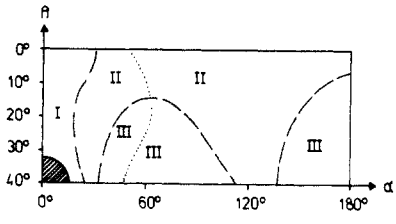

Figure 3. EH-calculated relative energetic order of the two lowest unoccupied orbitals in the model dimeric σ complex as a function of the torsional and interplanar angles α and β, respectively. The minute shaded region designates the geometry with through-space-determined order, i.e. $(\pi_3^+ - \sigma)$ lower than $(\pi_3^- + \sigma^*)$. All other geometries are characterized by the through-bond-determined order, i.e. $(\pi_3^- + \sigma^*)$ energetically lower than $(\pi_3^+ - \sigma)$. The actual splitting between these two LUMOs varies as follows: ≤0.4 eV (region I), 0.4–0.8 eV (II), ≥0.8 eV (III). The dotted line marks the energetic crossing of the symmetrical and antisymmetrical HOMO combinations with dependence on two angles α and β (c.f. Figure 2).

teraction.[14] The last two columns of Figure 1 show the correlation for the (photochemical) dissociation of dimeric σ complexes into two radical cations (E → F). Both the unsubstituted benzene and the 1,3,5-tripyrrolidinobenzene radical cation **1a**$^{\bullet+}$ (with D_{6h} and D_{3h} symmetry, respectively) have degenerate frontier orbitals. Thus, two Jahn–Teller distorted structures are to be expected for the tripyrrolidino as for the benzene radical cation.[2] Figure 4 shows the two MNDO-optimized geometries **9**$^{\bullet+}$**–I** and **9**$^{\bullet+}$**–II** of the 1,3,5-tris(dimethylamino)benzene radical cation, as a model for the tripyrrolidino derivative, together with the two highest occupied π orbitals and the MNDO-calculated charge densities. In terms of the single-determinant approximation, the following conclusions can be derived from the correlation diagram (Figure 1, columns E → F): Independent of energetic hierarchy, splitting, and symmetry of the two HOMOs, the electronic ground-state configuration of the dimeric σ complexes correlates directly and adiabatically with two identical Jahn–Teller distorted radical cations **9**$^{\bullet+}$**–II** with two singly occupied SOMOs Φ_3. The first electronically excited state of the dimeric σ complexes, for through-bond-determined order of the two LUMOs, likewise correlates, directly and adiabatically, with the two distinctly different Jahn–Teller distorted radical cations **9**$^{\bullet+}$**–I** and **9**$^{\bullet+}$**–II**.[15] Thus, both thermal and—energetically even more favorable—

(14) For the "classical" through-space-determined sequence, an electron would be promoted from the same HOMO (with virtually no σ/σ^* character) to a LUMO with high σ character. This is equivalent with a tightening of the central bond, i.e. corresponds to the formation of an intramolecular exciplex which would be less prone to dissociate.

(15) For the "classical" through-space-determined order of the two LUMOs, the first electronically excited configuration formally correlates with an electronically excited configuration of the two radical cations. If, on the other hand, configuration interaction is taken into account, this configuration likewise correlates with the ground state of the two different radical cations, **9**$^{\bullet+}$**–I** and **9**$^{\bullet+}$**–II**, although across a substantial energy barrier (due to the intersystem crossing interdict).

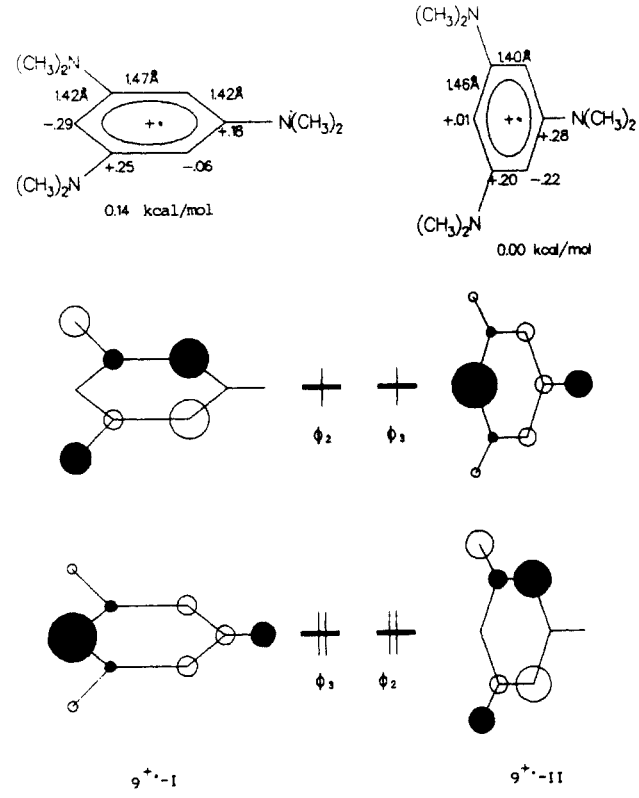

Figure 4. MNDO-calculated geometries, charge densities, relative energy, and highest occupied orbitals of the two Jahn–Teller distorted structures of 1,3,5-tris(dimethylamino)benzene radical cations, **9**$^{\bullet+}$**–I** and **9**$^{\bullet+}$**–II**, as a model for the unsubstituted 1,3,5-tripyrrolidin-1-ylbenzene radical cation **1a**$^{\bullet+}$.

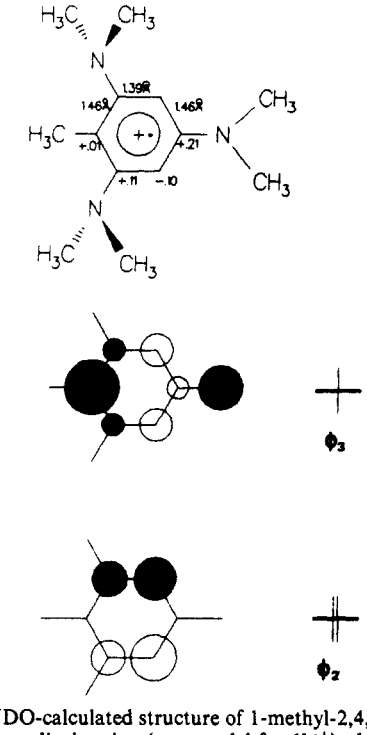

Figure 5. MNDO-calculated structure of 1-methyl-2,4,6-tris(dimethylamino)benzene radical cation (as a model for **1b**$^{\bullet+}$): bond lengths and charge densities (top) and highest occupied π orbitals (bottom).

photochemical dissociation into two radical cations are symmetry-allowed processes for the dimeric σ complexes **2** with through-bond-determined LUMO order. For a through-space-determined LUMO order, the photoreaction would be symmetry-forbidden.

Both the Jahn–Teller distorted forms of **9a**$^{\bullet+}$, as well as of **1a**$^{\bullet+}$, are planar. In structure II, the overall highest coefficient, and

hence spin density of the SOMO Φ_3, is located at C(1) which is freely accessible and is thus the predestined point of attack in dimerization, as well as in other radical reactions. Structure I, in contrast, is characterized by a relatively high coefficient at C(3) and C(5) (see Figure 4) which also are freely accessible and, hence, likely targets for radical attack. MNDO calculations demonstrate that, upon introduction of an alkyl substituent into the radical cation at C(1), the two neighboring dialkylamino groups are twisted almost 90° relative to the ring plane, leaving, e.g. for **1c**$^{\bullet+}$, structure **1c**$^{\bullet+}$**–II** as single energy minimum which is easily understood by qualitative arguments. The electronic configuration $\Phi_1^2\Phi_2^2\Phi_3^1$ again is characterized by an extremely high coefficient density at the alkyl-substituted ring carbon, as shown in Figure 5 for the 2-methyl-1,3,5-tris(dimethylamino)benzene radical cation. The reactive center, although favored electronically, appears sterically very well shielded by the alkyl substituent itself, and by the two, almost orthogonal NR_2 groups in α,α' position.

On the basis of these theoretical arguments, and with the assumption of kinetic control, the following predictions can be made concerning regioselectivity and relative reactivity of the two 1,3,5-tripyrrolidinobenzene radical cations **1a**$^{\bullet+}$ and **1c**$^{\bullet+}$; all of them have been validated experimentally (see above). Reaction of **1a**$^{\bullet+}$ with a sterically demanding second radical cation (which would directly yield the dimeric σ complex **2a**), hydrogen abstraction from a much less bulky solvent molecule, and reaction with the sterically least demanding O_2 are all equally facilitated at either C(1) in structure **1a**$^{\bullet+}$**–II** or C(3) and C(5) in structure **1a**$^{\bullet+}$**–I**. The radical cation **1c**$^{\bullet+}$, in contrast, where electronic direction allows for reaction only at the extremely shielded carbon C(1) may be attacked at this site but by sufficiently small reagents. Hydrogen abstraction from the solvent and O_2 addition thus are still practical and are indeed observed at the alkyl-substituted ring carbon exclusively. Dimerization at this site, being sterically impossible, is restricted to a nonalkylated ring position. Since this is very unfavorable electronically, dimerization of the ethyl-substituted radical cation **1c**$^{\bullet+}$ appears, kinetically, severely impeded relative to that of the unsubstituted **1a**$^{\bullet+}$, and its lifetime consequently is 1000 times longer.

Experimental Section

Melting points were determined on an Büchi SMP 20 apparatus in a silicon bath and are uncorrected. ^{1}H NMR spectra were obtained on a Varian A 60, T 60, Bruker MP 80 (CW), or a Bruker HX 90 E FT spectrometer. Chemical shifts are given in δ (ppm) relative to TMS as internal standard. UV spectra were obtained on a Cary 14 MP 50 spectrometer and MS spectra on a Varian MAT 711 spectrometer.

General Procedure for the Oxidation of 1,3,5-Tripyrrolidin-1-ylbenzenes 1 in either N_2 or O_2 Atmosphere with Exclusion of Light (for Results, See Table I). (A) In Nitrogen Atmosphere. A solution of **1** (1 mmol = 285 mg of **1a**, 299 mg of **1b**, 313 mg of **1c**, 327 mg of **1d**) in purified, freshly distilled CH_2Cl_2 (60 mL, in a flask carefully covered with aluminum foil) is flushed for 21 h with highest purity N_2 (deoxygenated, dried, and passed over potassium-coated charcoal). After that time, half of the solvent had evaporated. A solution of $AgNO_3$ (0.17 g, 1 mmol) in CH_3CN/CH_2Cl_2 (1:2 v/v, 15 mL, likewise thoroughly purged with N_2) was added under a slow N_2 stream: (a) within 10 s with vigorous stirring, the solution turning deeply red immediately; after 10 min of stirring, the precipitated amorphous silver was filtered off, the red filtrate was evaporated to dryness at ambient temperature, and the red crystalline residue was dried at 60 °C and analyzed by ^{1}H NMR; and (b) dropwise over a 6-h period and subsequently worked up as described.

(B) In Oxygen Atmosphere. The oxidation of **1a** was carried out as described above. The reaction mixture was flushed with O_2, however, and only half the solvent quantities was used. The $AgNO_3$ solution was added with a violent O_2 stream passed through the reaction mixture (evaporated solvent was replaced intermittently to keep the solvent volume constant), and the reaction was worked up rapidly as described above. The green, oily residue obtained upon evaporation was dried at 60 °C, yielding a green powder which was immediately analyzed by ^{1}H NMR. In contact with air moisture, the powder quickly turned oily again.

Preparative Oxidation of 1a–c to 6a, 7b, and 7c. 1-Oxo-2,4,6-tripyrrolidin-1-ylcyclohexadienylium Perchlorate (6a). A solution of $AgNO_3$ (0.34 g, 2 mmol) in CH_3CN (30 mL) was added dropwise within 2 h to a stirred solution of 1,3,5-tripyrrolidin-1-ylbenzene (**1a**) (0.57 g, 2 mmol) in CH_3CN (50 mL) and cooled to −5 °C with vigorous flushing with O_2. The solution turned dark green immediately, and amorphous silver was precipitated. The precipitate was filtered off, and ether (400 mL) was added to the filtrate. The dark green oil separated upon ether addition was extracted several times with water (total volume 800 mL). The aqueous extracts were filtered, and a saturated aqueous solution of sodium perchlorate (30 mL) was added dropwise to the filtrate, yielding crystalline **6a** (745 mg, 94%), mp 192 °C. Recrystallization from methanol yielded 605 mg **6a** (76%): mp 195–196 °C; ^{1}H NMR ($CDCl_3$) δ 5.30 (s, 2 H, 3,5-H), 4.0–3.6 (m, 12 H, α-Pyr-CH_2), 2.2–1.8 (m, 12 H, β-Pyr-CH_2). Anal. Calcd for $C_{18}H_{26}ClN_3O_5$: C, 54.06; H, 6.55; Cl, 8.86; N, 10.51. Found: C, 54.17; H, 6.70; Cl, 9.09; N, 10.80.

3,3′-Dimethyl-2,2′,4,4′,6,6′-hexapyrrolidin-1-yl-1,1′-bicyclohexadienylium Peroxide Diperchlorate (7b). A solution of $AgNO_3$ (0.34 g, 2 mmol) in CH_3CN/CH_2Cl_2 (1:1 v/v, 10 mL) was added dropwise to a stirred solution of 1-methyl-2,4,6-tripyrrolidin-1-ylbenzene (**1b**) (0.6 g, 2 mmol) within 6 h at ambient temperature, and the reaction mixture was vigorously flushed with O_2. The amorphous silver precipitate was filtered off, the filtrate was evaporated at ambient temperature, and the oily residue was dissolved in water (10 mL) and purified by column chromatography at molecular sieve GT 10. A yellow fraction which was eluted first was discarded; a second green fraction was collected, and a saturated aqueous solution of sodium perchlorate was added. The yellow precipitate was filtered off and dried at 70 °C, yielding **7b** (130 mg = 16%): mp 177 °C; ^{1}H NMR ($CDCl_3$) δ 4.63 (s, 2 H, 5,5′-H), 4.0–3.6 (m, 24 H, α-Pyr-CH_2), 2.2–1.8 (m, 24 H, β-Pyr-CH_2), 1.73 (s, 6 H, CH_3). Anal. Calcd for $C_{38}H_{58}Cl_2N_6O_{10}$: C, 55.00; H, 7.04; Cl, 8.54; N, 10.13. Found: C, 53.97; H, 7.01; Cl, 8.67; N, 9.95.

3,3′-Diethyl-2,2′,4,4′,6,6′-hexapyrrolidin-1-yl-1,1′-bicyclohexadienylium Peroxide Diperchlorate (7c). 1-Ethyl-2,4,6-tripyrrolidin-1-ylbenzene (**1c**) (0.63 g, 2 mmol) in CH_2Cl_2 (30 mL) was converted to the peroxy complex **7c** with $AgNO_3$ (0.34 g, 2 mmol) in CH_3CN/CH_2Cl_2 (1:1 v/v, 10 mL) as described for **7b**. **7c**: yield 210 mg (25%); mp 175 °C; ^{1}H NMR ($CDCl_3$) δ 4.76 (s, 2 H, 5,5′-H), 4.0–3.4 (m, 24 H, α-Pyr-CH_2), 2.2–1.7 (m, 28 H, β-Pyr-CH_2 and α-Et-CH_2), 0.77 (t, 6 H, β-Et-CH_3). Anal. Calcd for $C_{40}H_{62}Cl_2N_6O_{10}$: C, 56.00; H, 7.28; Cl, 8.26; N, 9.79. Found: C, 56.07; H, 7.38; Cl, 8.42; N, 9.62.

Oxidation of d_3-1a. (a) 1,3,5-Tripyrrolidin-1-ylbenzene-d_3 (d_3-1a). A suspension of **1a** (5.0 g, 17.5 mmol) in CH_3OD (10–20 mL; acidified with 2 drops of DCl/D_2O) was stirred for 3–9 h at ambient temperature, the solvent was stripped off, and the residue was dried in high vacuo. This procedure was repeated four times, and the percentage of H/D exchange was determined by ^{1}H NMR as 93%. The dark green product was purified by recrystallization from C_6H_6/SiO_2, and the resulting beige-colored crystals were dried in high vacuo, yielding d_3-**1a** (3.15 g, 63%), mp 179–180 °C.

(b) A solution of $AgNO_3$ (1.0 g, 5.9 mmol) in CH_2Cl_2/CH_3CN (3:1 v/v, 20 mL) was added dropwise to the O_2-flushed solution of 72% core deuterated d_3-**1a** (see above, 1.7 g, 5.9 mmol) in CH_2Cl_2. After completion of the oxidation, CH_2Cl_2 was distilled over (where the resulting H_2O was taken along azeotropically). The distillate was cooled to −78 °C, CH_2Cl_2 was then removed with a pipet, and the residue was allowed to warm to ambient temperature, yielding two phases. CH_2Cl_2 again was removed with a pipet, and the remaining drop of water was investigated by MS (70 eV, 0.8 mA, source temperature 445 k) to give a percentage composition of H_2O (47%), HOD (40%), and D_2O (13%).

Dissociation of the Dimeric σ-Complexes 2 in either N_2 or O_2 Atmosphere with Exclusion of Light (for Results, See Table II). (A) Dissociation of 2,2′,4,4′,6,6′-Hexapyrrolidin-1-yl-1,1′-bicyclohexadienylium Perchlorate (2a). A solution of **2a** (385 mg, 0.5 mmol) in CH_3CN (30 mL)—with or without **1a** (285 mg, 1 mmol) added—was flushed with highest purity N_2 and O_2, respectively (for reaction times and temperatures, see Table II). After completion of the reaction, the solution was evaporated to dryness, and the residue was dried. Formation of **6a** was established from a sample of the dried residue by UV. If the reaction was carried out in the presence of **1a**, the dry residue was extracted with ether in a Soxhlet apparatus until ^{1}H NMR showed no **1a** to be present any longer in the solid residue. The residue was then dissolved in CH_3CN (10 mL) and concentrated KOH (10 mL) was added. The precipitated beige product mixture [containing deprotonated **2a**, i.e. 2,2′,4,4′,6,6′-hexapyrrolidin-1-yl-1,1′-biphenyl (**4a**) as well as deprotonated **3a**, i.e. tripyrrolidinobenzene **1a**] was dried and the percentage composition determined by ^{1}H NMR. For reactions without addition of **1a**, the crude residue was deprotonated directly without ether extraction.

(B) Dissociation of the 3,3′-Dialkyl-2,2′,4,4′,6,6′-hexapyrrolidin-1-yl-1,1′-bicyclohexadienylium Complexes 2b–d. The reactions were carried out with 0.5 mmol of dimeric σ complex (**2b**, X = BF_4, R = CH_3, 386 mg; **2c**, X = ClO_4, R = C_2H_5, 413 mg; **2d**, X = ClO_4, R = $CH(CH_3)_2$, 427 mg) in purified CH_2Cl_2 (30 mL), with or without **1a** added. To ensure absolute exclusion of oxygen for the N_2 reactions, the educt **2** and the solvent (with or without **1a** added) were each subjected separately

three to four times to a freeze–thaw procedure with highest purity N_2 (deoxygenated, dried, and passed over potassium-coated charcoal). The CH_2Cl_2 solvent or solution was added to the dimeric σ complex, and the reaction mixture was flushed with highest purity N_2 or O_2 for the period given in Table II (25 °C, strict exclusion of light). After completion of the reaction, the solvent was evaporated at ambient temperature, the residue was dried, and the percentage composition of the products was determined by UV and ^1H NMR as described in A.

UV Spectroscopic Determination of the Half-Periods of the Dimeric σ Complexes 2b–d at Ambient Temperature (for Results, See Table IIIA). (A) With Exclusion of Light. Purified acetonitrile was purged for 60 min with highest purity N_2 in a 1-cm UV cuvette covered with aluminum foil and equipped with a stopcock; **2** was added with continued N_2 flushing, the stopcock was closed, and UV measurement commenced immediately. The initial concentration of **2** was determined retrospectively from the three isosbestic points between 550 and 230 nm, and the progress of the reaction was followed by monitoring extinction at 400 nm.

(B) With Intermittent Exposure to Daylight. The reaction was carried out as described in A, with the closed cuvette intermittently being exposed to daylight (1–2 s each time).

^1H NMR Spectroscopic Determination of the Half-Periods of the Dimeric σ Complexes 2b–d, with or without π Donors Added (at 30 °C, with Exclusion of Light (for Results, see Table IIIB). To a solution of 0.1 mmol of the dimeric σ complexes (perchlorates) (**2b**, R = CH_3, 798 mg; **2c**, R = C_2H_5, 826 mg; **2d**, R = $CH(CH_3)_2$), 854 mg) in CD_3CN/CH_2Cl_2 (1:1 v/v, 1 mL) was added 0.15 mmol of **1** (**1a** = 43 mg, **1b** = 45 mg, **1c** = 49 mg, and 1,3,5-tripiperidin-1-ylbenzene, 49 mg), respectively. Decomposition of the educts **2** (30 °C, with exclusion of light) was followed by ^1H NMR, and the individual percentage composition was calculated from the integrals.

Flash Photolysis Measurements. A conventional flash photolysis apparatus[9a] was used to follow the decay of radicals $\mathbf{1c}^{\bullet+}$ produced by excitation (λ_{exc} > 400 nm) of ca. 10^{-5} M solution of **2c** (X = ClO_4) in acetonitrile (Merck reagent grade); observation at λ_{obs} = 800 nm, pathlength of the cuvette 10 cm. Oxygen was removed by bubbling pure nitrogen (O_2 content < 6 ppm) for 30 min. The influence of oxygen on the decay of $\mathbf{1c}^{\bullet+}$ was studied in air-saturated solution.

A home-built laser flash apparatus with signal averaging[9b] (time resolution ca. 0.25 μs) was used to measure the quantum yield of photodissociation of **2c** and the transient spectra of intermediates and to follow the reaction between $\mathbf{1c}^{\bullet+}$ and **1a** or **1c**, respectively (concentrations of **1a**, from 5×10^{-4} to 1×10^{-2} M); optical pathlength of the (flow through) cuvette 1 cm, concentration of **2c** ca. 10^{-4} M.

Acknowledgment. We express our thanks to P. Fischer for helpful discussions and also for the translation of this contribution. Financial support by the Deutsche Forschungsgemeinschaft and the Fonds der Chemischen Industrie is gratefully acknowledged.

Laser Flash Photolysis of 9-Fluorenol. Production and Reactivities of the 9-Fluorenol Radical Cation and the 9-Fluorenyl Cation

Robert A. McClelland,*[1a] N. Mathivanan,[1a] and Steen Steenken[1b]

Contribution from the Department of Chemistry, University of Toronto, Toronto, Ontario, Canada M5S 1A1, and the Max-Planck-Institut fur Strahlenchemie, D-4330 Mulheim, West Germany. *Received December 1, 1989*

Abstract: Two recent flash photolysis investigations of 9-fluorenol (FOH) in aqueous methanol have reached conflicting conclusions regarding the spectrum and lifetime of the 9-fluorenyl cation (F^+). Gaillard, Fox, and Wan (GFW) (*J. Am. Chem. Soc.* **1989**, *111*, 2180) attributed to F^+ a transient at 640 nm with lifetimes in the microsecond range, while Mecklenburg and Hilinski (MH) (*J. Am. Chem. Soc.* **1989**, *111*, 5471) concluded that F^+ was the transient they observed at 515 nm which formed and decayed in <20 ps. MH ascribed the 640-nm transient to the 9-fluorenol radical cation ($FOH^{\bullet+}$). In the present study $FOH^{\bullet+}$ has been produced in aqueous trifluoroethanol and in aqueous acetonitrile by reacting FOH with $SO_4^{\bullet-}$ produced by 248-nm photolysis of the $S_2O_8^{2-}$ ion. The $FOH^{\bullet+}$ so formed has absorptions with λ_{max} at 395, 595, and 645 nm and decays with lifetimes of 10–100 μs. We conclude therefore that the 640-nm transient is $FOH^{\bullet+}$, and not F^+. $FOH^{\bullet+}$ forms in the direct photolysis by two-photon ionization, a conclusion reached on the basis of the quadratic dependency of the 640-nm absorbance on the intensity of the exciting light. The radical cation of fluorene has been produced in aqueous acetonitrile as well, both by photoionization and by reaction with $SO_4^{\bullet-}$; this species has λ_{max} at 365, 590, and 645 nm, and a lifetime similar to that of $FOH^{\bullet+}$. The 515-nm transient is observed as a relatively long-lived species (30 μs) upon photolysis of FOH in 1,1,1,3,3,3-hexafluoroisopropyl alcohol (HFIP). This transient is not quenched by oxygen, its decay is accelerated by nucleophiles such as water and trifluoroethanol, and 1,1,1,3,3,3-hexafluorisopropyl 9-fluorenyl ether is obtained as the only product of photolysis. We conclude therefore that the 515-nm transient is the ground-state 9-fluorenyl cation, which has also been observed by MH in aqueous methanol where its lifetime is <20 ps. The remarkably weak nucleophilicity of HFIP is further demonstrated by kinetic and product experiments that show that F^+ undergoes electrophilic substitution of benzene in competition with capture by this solvent.

Wan and co-workers have found that 9-fluorenol (FOH) undergoes an efficient photosolvolysis in methanol or aqueous methanol resulting in the production of 9-methoxyfluorene (FOMe).[2a,b] A mechanism was proposed with an intermediate 9-fluorenyl cation (F^+) produced by photoheterolysis of excited FOH. The relative ease of formation of the cation even with the poor leaving group OH^- was attributed to the enhanced reactivity of excited states leading to $4n$ π systems.[2]

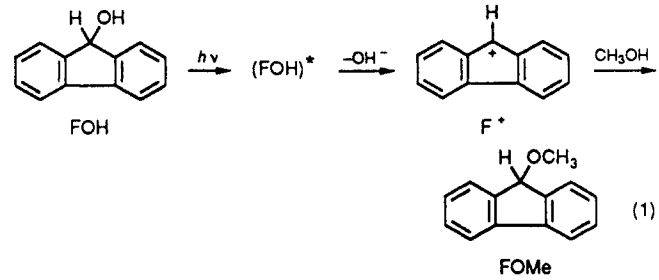

(1)

This work has prompted investigations employing time-resolved methods. Gaillard, Fox, and Wan (GFW), using nanosecond laser

(1) (a) University of Toronto. (b) Max-Planck-Institut.
(2) (a) Wan, P.; Krogh, E. *J. Chem. Soc., Chem. Commun.* **1985**, 1027. (b) *J. Am. Chem. Soc.* **1989**, *111*, 4887. (c) Wan, P.; Krough, E.; Chak, B. *J. Am. Chem. Soc.* **1988**, *110*, 4073.

0002-7863/90/1512-4857$02.50/0